Ruprecht 55: an OB association at the edge of our Galaxy

Guillermo Bosch,[1]⋆†‡ Rodolfo Barbá,[1]‡§ Nidia Morrell,[1]†‡§ Virpi Niemela,[1]†‡¶
Pablo Ostrov,[1]‡ Marcelo Arnal,[1,2]§ Cristina Cappa,[1,2]§ Ricardo Morras[1,2]§
and Guillermo Giménez de Castro[3]

[1]*Facultad de Ciencias Astronómicas y Geofísicas, Universidad Nacional de La Plata, Paseo del Bosque, (1900) La Plata, Argentina*
[2]*Instituto Argentino de Radioastronomía, CC 5, (1894) Villa Elisa, Argentina*
[3]*CRAAE: (Mackenzie, INPE, USP, UNICAMP), Instituto Presbiteriano Mackenzie, Rua de Consolação 896, 01302-000 S. Paulo, SP, Brazil*

ABSTRACT

We present new spectroscopy in the optical range and 21-cm H I data covering the Ruprecht 55 (Ru 55) field in the Puppis window where several authors have proposed the existence of one (or two) clusters.

We have determined new MK spectral types for about 50 stars in the region, finding 43 OB-type stars among them. LS 985 was found to be an O9 V + O9.5 III binary and it is the earliest type of star in our observed sample.

We have identified a stellar OB association (Ru 55), which is most likely related to a depletion detected in our H I data, as: (i) they are located at the same distance (6 kpc), within observational errors; (ii) both have similar radial velocities ($\sim$67 km s^{-1}); (iii) current OB stars could have provided the energy needed to blow the cavity; (iv) the dynamical time-scale for the hole buildup matches the age estimated for the earliest OB stars; and (v) LS 985 might be responsible for ionizing the H I cavity inner walls close to it.

Key words: stars: early-type – ISM: bubbles – ISM: kinematics and dynamics – open clusters and associations: individual: Ruprecht 55 – Galaxy: structure.

1 INTRODUCTION

OB associations are natural tracers of the spiral structure of galaxies such as our Milky Way. Although there is increasing knowledge of the local neighbourhood associations (de Zeeuw et al. 1999) it is still very difficult to obtain information of stellar groupings beyond some kiloparsecs from us. The fact that the Sun lies in the very Galactic plane makes it almost impossible to see through the nearest neighbouring spiral arms (i.e. Perseus outwards and Sagittarius inwards).

However, there are specific directions in the sky which we can point at in order to peek at more distant OB associations. One of these, the so-called 'Puppis window' is located in the third quadrant ($230^\circ < l < 255^\circ$). In this direction we can trace the extension of the Perseus arm in the outer regions of our Galaxy, thanks to the relatively low extinction between spiral arms. Furthermore, this window allows the galactic structure to be probed even further, as far as the

'15-kpc arm' (Stetson & Fitzgerald 1985). Yet, the downside is that everything is projected on the observed field, and it turns out to be quite difficult to reliably identify the membership of individual stars in a particular group. It is therefore necessary to gather information from photometry (magnitudes and colours), spectroscopy (intrinsic colours and kinematics) and radio wavelength observations (interstellar matter).

The first extensive study dedicated to the detection of OB stars in the Puppis window was performed by Orsatti (1992, hereafter O92) covering some 40 deg^2 centred on $l = 248^\circ$, $b = -1^\circ\!.5$. Among other findings, it was noticed that a number of OB+ stars seemed to group around the location of the Ruprecht 55 (Ru 55) star cluster. This cluster has been the subject of a photographic photometry search for members by Dodd & Ellery (1980, hereafter DE80), and photoelectric photometry study by Orsatti (1995, hereafter O95). O95 suggests that there are two clusters lying in the direction towards Ru 55, which she labelled as Ru 55 A and Ru 55 B, lying 4.2 and 7.5 kpc away from the Sun, respectively. This would place Ru 55 A in the Perseus arm and Ru 55 B in the 15-kpc arm. These distances make any kinematical study based on proper motions almost impossible for the facilities currently available.

The goal of this study is to investigate the existence of a stellar cluster or association where suggested by Ruprecht and collaborators (Alter et al. 1970) and therefore to estimate its location within

⋆E-mail: guille@fcaglp.unlp.edu.ar
†Visiting Astronomer, CTIO.
‡IALP, Instituto Astrofísico de La Plata.
§Member of the Carrera del Inv. Científico, CONICET, Argentina.
¶Member of the CIC, Prov. de Bs. As., Argentina.

our Galaxy and its evolutionary stage. In order to tackle this problem we started a programme to obtain CCD photometry and medium resolution spectroscopy of the earliest-type star candidate members of Ru 55, and to compare their kinematics with that of the neutral hydrogen in its neighbourhood.

2 OBSERVATIONS AND DATA REDUCTION

2.1 Photometry

Observations were carried out using the Curtis Schmidt Telescope at the Cerro Tololo Inter-American Observatory (CTIO, Chile) during three nights in 1994 March. A Thompson 1024×1024 CCD was used, covering a field of view of 31 arcmin on a side, with a pixel scale of 1.83 arcsec pixel^{-1}. Seven fields including Ru 55 and its surrounding area were observed using *U*, *B*, *V* and *R* filters, tied to the SA104 standard star field (Landolt 1992). Aperture photometry was performed using the DAOPHOT package (Stetson 1987) within IRAF.[1]

2.2 Spectroscopy

Spectroscopic observations of candidates selected from the literature and our CCD photometry were obtained on three observing runs. The selection was based on the magnitude $V < 13.5$, and the reddening-free parameter $Q < -0.4$, although the observed sample is not complete. Medium resolution (0.45 Å px^{-1}) spectroscopy was obtained at the 2.15-m telescope at the Complejo Astronómico El Leoncito (CASLEO) using the REOSC échelle Cassegrain spectrograph[2] in 1994 January and with the Shectman–Heathcote two-dimensional photon-counting detector on the Cassegrain spectrograph attached to the 1-m telescope at CTIO in 1994 February. Low-resolution (1.65 Å px^{-1}) spectroscopy was obtained with the REOSC spectrograph in simple dispersion mode at CASLEO in 1996 February. Spectra were reduced using standard procedures with IRAF.

2.3 Radio

Neutral hydrogen line observations at 1420 MHz were made using the 30-m dish of the Instituto Argentino de Radioastronomía (IAR) at Villa Elisa (Argentina). A full-sampled raster map in galactic coordinates covering the area defined by $247°0 \leqslant l \leqslant 252°0$ and $-1°0 \leqslant b \leqslant +5°0$, centred at the optical position of Ru 55, was observed in 1994 March. The half power beamwidth (HPBW) of this antenna is 30 arcmin at that frequency. The receiver was used in its total power mode. The system temperature against cold sky was about 35 K. A 1008-channel autocorrelator was used as the back end. The bandwidth of 5 MHz yields a velocity resolution of 1.27 km s^{-1} and a velocity coverage of about 1060 km s^{-1}. The integration time of each point was 1 min, yielding a rms noise level of individual profiles of 0.16–0.21 K in main beam brightness temperature. The brightness temperature scale was derived from observations of the calibration point S9 (Williams 1973). The overall brightness temperature scale is accurate to within 3–4 per cent.
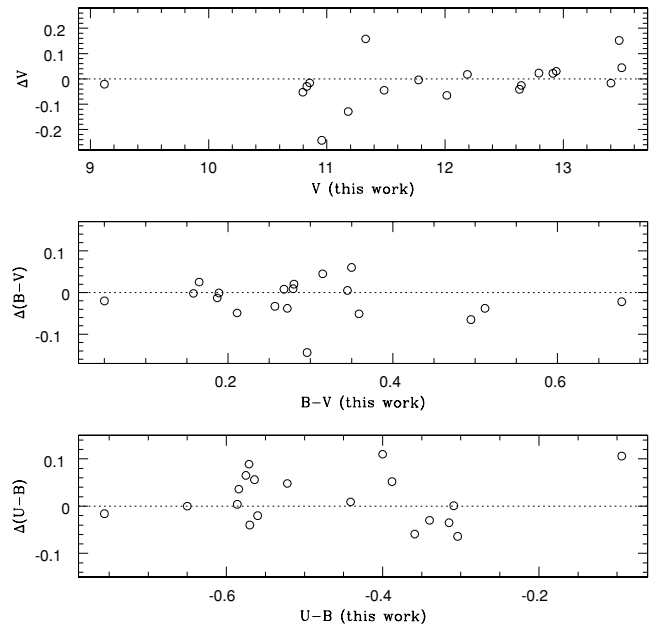

Figure 1. Comparison between the ($U–B$), ($B–V$) colours and *V* magnitudes obtained in our study and those available in the literature.

3 RESULTS

3.1 Comparison with previous photometric studies

UBV magnitudes were derived for stars in the region from our CCD frames. Previously, O92 and DE80 presented photoelectric and photographic photometry in the same region. For stars in common with those studies we have compared the values for *V* magnitudes and *B–V*, *U–B* colours finding no evidence of systematic differences between them (see Fig. 1). The star DE 32 ([O92] 390) was measured to have $V = 11.17$, 10.75, and 11.33 in DE80, O92 and the present paper, respectively. These discrepancies (also pointed out in O95) could indicate intrinsic variability of the star which is also suggested by the variable emission line spectrum (see Section 3.2). Table 1 lists the stars in the field of Ru 55 observed spectroscopically in this investigation. The photometric information recorded in this table is as follows in order of availability and preference: CCD photometry (this paper), photoelectric and photographic photometry from DE80 and O92.

3.2 Spectral classification

Spectral classification is required in order to obtain reliable intrinsic colours needed to correct for interstellar reddening and absorption. We have therefore obtained high signal-to-noise spectra for 44 early-type stars among the probable members of Ru 55. We derived spectral types from our data (listed in Table 1) according to the classification criteria described by Walborn & Fitzpatrick (1990). Comments about particular characteristics of these objects are also included in Table 1. Fig. 2 only includes spectra of stars mentioned in the text. The full set of figures showing spectra for all stars included in Table 1 is available in the electronic version of the article on *Synergy*.

We have found an O-type double-lined binary, LS 985 (which we will discuss further below), a majority of early B-type stars (some of them of luminosity classes I and II) and a few foreground late-type stars.

Table 1. Photometric and spectroscopic information for individual stars analysed in this work. Column 1 lists the star identification where LS indicates stars in the Luminous Star Catalogue (Stephenson & Sanduleak 1971), DE indicates stars in DE80, [O92] labels stars according to O92 and S labels stars from this work, following GSC2.2 nomenclature. Columns 2 and 3 show the stellar celestial coordinates in the J2000 frame, columns 4–6 list the *UBV* magnitude and colours. The MK spectral classification is listed in column 7 and their corresponding intrinsic $(B-V)$ colour is shown in column 8. LSR radial velocities are listed in column 9 and their corresponding errors (with the number of spectra available between parentheses) in column 10. The derived DM are listed in column 11.

ID	α_{2000}	δ_{2000}	V	$(B-V)$	$(U-B)$	Spectral type	$(B-V)_0$	V_r	ΔV_r	DM
LS 987 (DE 25)	08 12 10.0	−32 34 05	8.56	0.41	−0.50	B2.5 Iab	−0.15	72	6 (8)	13.2
HD 68552 (LS 985)	08 11 42.1	−32 09 13	9.12	0.05	−0.76	O9.5III + O9Ve	−0.31	78	71 (3)	13.2
LS 953	08 04 28.6	−30 58 21	10.45	0.25	−0.79	Be pec	−0.26	50	6 (3)	13.3
LS 994 (DE 30)	08 12 32.5	−32 34 34	10.80	0.31	−0.59	B1 IIe	−0.26	63	6 (7)	14.4
LS 988 (DE 31)	08 12 11.8	−32 39 20	10.83	0.35	−0.65	B1 II	−0.26	69	6 (7)	14.3
LS 991 (DE 29)	08 12 21.0	−32 35 03	10.85	0.28	−0.58	B1 IV	−0.26	67	23 (7)	13.0
DE 13	08 12 44.3	−32 38 53	10.96	0.16	−0.31	B9 V	−0.07	10	34 (6)	10.0
DE 23	08 12 27.0	−32 39 41	11.18	0.28	−0.39	B3 V	−0.20	36	6 (7)	11.3
LS 989 ([O92] 390,DE 32)	08 12 12.5	−32 28 14	11.33	0.34	−0.57	B0 IIIe	−0.29	68	6 (6)	14.5
LS 970	08 08 39.3	−33 04 51	11.39	0.15	−0.97	B0.5 IV	−0.28	−21	19 (2)	14.3
[O92] 366	08 09 46.6	−32 14 52	11.48	0.26	−0.57	B2-3 III	−0.22	34	6 (2)	13.5
S 1330122882	08 12 20.8	−32 47 33	11.59	0.22	−0.45	B3 V	−0.20	...	...	11.9
LS 961	08 05 56.9	−33 00 22	11.62	0.61	−0.34	B1 III	−0.26	5	18 (1)	13.3
LS 1003 (DE 34)	08 12 58.0	−32 34 45	11.78	0.19	−0.57	B2 IV	−0.24	61	6 (6)	13.5
[O92] 372	08 10 18.7	−31 07 21	11.80	...	...	B2-3 III Ve	−0.22	62	23 (2)	...
LS 963 ([O92] 330)	08 06 11.6	−33 16 42	11.88	0.67	−0.27	B1 II	−0.26	108	50 (3)	14.4
LS 999 (DE 33)	08 12 49.6	−32 29 34	12.02	0.19	−0.44	B3 V + B5-7	−0.20	30	135 (6)	12.4
DE 26	08 12 22.7	−32 30 22	12.19	0.17	−0.30	B9 V	−0.07	1	7 (6)	11.3
LS 1009	08 13 42.5	−32 53 17	12.27	0.09	−0.70	B2-3 III–V	−0.22	38	20 (3)	14.1
[O92] 388	08 11 53.3	−32 23 49	12.40	0.35	−0.42	B3-5 V	−0.19	52	8 (6)	12.2
[O92] 351	08 08 03.9	−32 13 29	12.45	0.97	−0.20	Be pec	−0.26	56	24 (3)	13.0
S 133012255	08 11 53.8	−32 17 52	12.52	0.75	−0.17	G0 V	0.58	...	...	7.6
DE 35	08 12 20.3	−32 35 06	12.63	0.27	−0.52	B1 IV	−0.26	64	12 (3)	14.8
DE 36	08 12 21.3	−32 35 11	12.64	0.21	−0.56	B1 V	−0.26	71	6 (8)	14.4
DE 10	08 12 23.8	−32 29 41	12.79	0.36	−0.09	B9 V	−0.07	28	14 (4)	11.3
[O92] 349	08 08 02.8	−31 35 46	12.83	0.63	−0.34	B1 IIIe	−0.26	108	6 (2)	14.5
[O92] 358	08 08 54.5	−31 48 09	12.83	0.68	−0.43	B2-3 III–Ve	−0.22	24	15 (2)	12.8
S 13303211856	08 12 50.4	−32 17 12	12.85	0.29	−0.48	B2.5 V	−0.22	...	...	13.3
[O92] 387 (DE01)	08 11 45.0	−32 32 46	12.91	0.50	−0.31	B2 III–V	−0.22	72	9 (7)	13.4
[O92] 383	08 11 10.0	−32 33 31	12.94	0.27	−0.56	B2 III–V + B3	−0.24	75	158 (2)	14.5
[O92] 348	08 08 02.2	−31 24 09	13.03	0.43	−0.14	B3 V	−0.20	46	8 (5)	12.7
[O92] 379	08 10 48.6	−32 02 27	13.08	0.58	−0.15	B3-5 III–Ve	−0.19	57	13 (2)	12.8
S 13303211827	08 11 30.1	−32 15 31	13.18	0.30	−0.48	B2.5 V	−0.22	...	...	13.6
[O92] 376	08 10 29.5	−32 30 21	13.20	0.43	−0.48	B2 III–V	−0.24	73	16 (1)	14.2
S 1330122206	08 13 32.1	−32 23 22	13.36	0.16	−0.41	B2 V	−0.24	...	...	14.6
[O92] 347	08 07 47.9	−32 24 05	13.37	0.88	−0.28	B1 V	−0.26	41	6 (1)	13.0
S 1330122143	08 11 22.6	−32 21 22	13.39	0.46	−0.54	B2 IV	−0.24	...	...	14.3
[O92] 368	08 09 58.4	−32 32 01	13.40	0.68	−0.34	B3-5 V	−0.19	78	6 (2)	12.1
S 1330122143	08 11 22.7	−32 21 24	13.41	0.30	−0.50	B2 IV	−0.24	...	...	14.8
S 13303211460	08 09 43.7	−32 04 37	13.43	0.36	−0.48	B2 III–V	−0.24	...	...	14.7
DE 04	08 12 10.4	−32 30 27	13.47	0.30	−0.40	B2 Vne	−0.24	85	25 (5)	14.3
S 1330122754	08 11 35.5	−32 42 37	13.48	0.42	−0.49	B2 V	−0.24	...	...	13.9
[O92] 381	08 11 03.2	−32 45 43	13.49	0.51	−0.36	B3 III	−0.20	83	8 (2)	14.3
[O92] 359	08 08 56.1	−32 11 56	13.87	0.52	−0.18	B2-3 III–Ve	−0.22	47	10 (1)	14.3
S 133012232510	08 12 13.8	−32 53 51	14.17	0.10	−0.87	A0 V	−0.02	...	...	13.2

Among the most luminous stars in the observed sample, we find one B-type supergiant (LS 987, see Fig. 2) and three B1-type stars of luminosity class II. One of the latter (LS 994) shows Balmer lines which are partially filled with emission, also observable in He I 5015 and 5876 Å. From the analysis of three medium-resolution spectra of LS 963 (B1 II) we determined that this star shows variable radial velocity (see next section).

Among the giant stars, the spectroscopic double-lined binary LS 985 shows weak emission in Hβ (Fig. 3). This is the only O-type star detected in the area, and it is also a visual binary with 2.1-arcsec separation and *V* magnitudes of 9.7 and 10.0 for both components, respectively (cf. Dommanget & Nys 2002). Curiously, LS 985 has been classified as B5 Ib/II in the Michigan Spectral Survey (Houk 1982) and B1 V (Garrison, Hiltner & Schild 1977). Those classifications indicate no detection of He II absorption lines. Our spectra of LS 985 were obtained with a slit of 2.5 arcsec in width, and a seeing about 2–3 arcsec, therefore both components of the visual binary were on the slit. As we will discuss in the next section, LS 985 shows variable radial velocities among its spectral features but with the available spectrographic material it
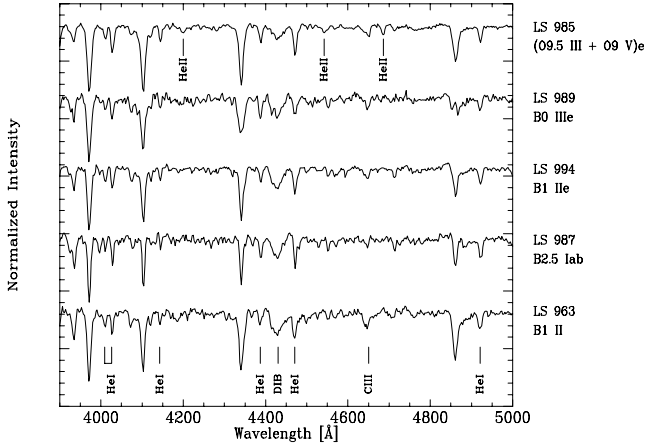
Figure 2. Sample spectra of stars in Ru 55 whose features are mentioned in the text. The complete set of spectra is available in the electronic version of the article on *Synergy*.

is not possible to specify how many stars compose this multiple system.

LS 989 (DE 32) is an early-B giant showing emission in Balmer and He I lines (Fig. 2). For example, He I 4471 Å and He I 4922 Å are partially filled by emission, easily seen when they are compared with He I 4387 Å. The intensity and shape of the Hβ emission is variable over a few days scale.

We identified several Be stars in the sample (10 out of 42). In particular, two of these are classified as Bep: LS 953 (Fig. 4) and [O92] 351 (Fig. 5). LS 953 displays strong Hβ emission with two barely resolved peaks, also present in Fe II multiplet 42. The absorption profiles are significantly broadened by rotation. [O92] 351 shows a noticeable Hβ emission superimposed on a continuum with weak absorptions of H, He I at shorter wavelengths, and many faint emissions of Fe II and He I. Also, [O92] 351 exhibits $(V - Ks) = 3.31$ (*Ks* magnitude from the Two Micron All Sky Survey (2MASS) Point Source Catalogue;[3] Cutri et al. 2000) indicating a possible intrinsic infrared excess of this source compared with normal $(V - Ks)$ colours for B-type stars (-0.9 for B0 to -0.2 for B9; Johnson 1966).

3.3 Stellar radial velocities

Binarity imposes a strict condition on the observation process followed to obtain radial velocities: repetition. No single calculation of a stellar radial velocity is to be fully trusted, unless subsequent monitoring confirms it. The large amounts of telescope time involved in this unavoidably delay the outcome of reliable findings. Table 1 lists our determinations of stellar radial velocities for a set of stars in the Ru 55 field, referred to the local standard of rest (LSR). These were converted from heliocentric velocities assuming the motion of the Sun with respect to the LSR to be 20 km s^{-1} in the direction $\alpha = 18^h$, $\delta = +20°$. Individual radial velocities were determined for each spectral feature by fitting Gaussian profiles to each absorption (or emission) feature in the stellar spectra in order to check for systematic differences among different ions – another flag of binarity –

and averaged to obtain the stellar radial velocity. The uncertainty in this average value indicates ΔV_r when only one observation is available. When two or more radial velocity determinations are performed, ΔV_r reflects the dispersion among these. There is, however, a minimum uncertainty in the determination of the centroid of a spectral feature which is approximately one tenth of the spectral resolution which, for this case, is ~6 km s^{-1}. The number of spectra available for each star is given in parentheses in column 10 of Table 1. Analysing the radial velocities derived from medium-resolution spectra we discovered three stars with composite spectra, four stars whose radial velocity variations suggest single-line spectroscopic binary nature, and two stars with probable variable radial velocity. Of the stars exhibiting composite spectra, we would suggest that LS 999 and [O92] 383 are double-lined spectroscopic binaries. The multiple nature of the O-type star LS 985 might be more complex, as mentioned in the previous section. This object is a visual double with components of very similar brightness separated by 2.1 arcsec. From our radial velocity determinations we cannot assert whether we are dealing with a double-lined spectroscopic binary or a higher multiplicity system. From the set of three observations, two of these show absorption lines that can be deblended in two components with radial velocities of about 0 and 155 km s^{-1}. If both components are of similar mass, we can guess a systemic velocity of about 78 km s^{-1}. The remaining spectrum of LS 985 shows no line splitting, with a radial velocity of 59 km s^{-1}. The existence of further components in the system cannot either be inferred or ruled out.

4 DISTANCES AND KINEMATICS

4.1 Spectroscopic parallaxes

The distance to the stars is determined using the method of spectroscopic parallax. From our determination of spectral types, we obtain the colour excesses $E(B–V)$ using the spectral type to intrinsic colours calibration from Schmidt-Kaler (1982). We assume for R_V a canonical value of 3.1, and then we correct our V photometry for extinction, $V_0 = V–3.1\,E(B–V)$. Also, the visual absolute magnitudes for the corresponding spectral type are taken from Schmidt-Kaler (1982), through bilinear interpolation for spectral type and luminosity class. For the two Be peculiar stars we arbitrarily adopt, as an upper limit, the colours and magnitude of a B1 III star. Previous colour excesses were derived purely from photometric data and we have checked for the presence of any systematic difference between them and the excesses obtained from the spectral classification. As can be seen in Fig. 6, we detect a slight (~0.05 mag) systematic overestimate of $E(B–V)$ from photometric data, most probably due to the limited information provided by the OB+, OB, OB− classification from objective prism spectroscopy.

The upper left-hand panel of Fig. 7 presents the histogram of the distribution of distance moduli (DM) for the observed stars. Two clusterings are apparent, identified by different strip patterns, at roughly $V_0 - M_V \sim 13.4$ (4.8 kpc) and $V_0 - M_V \sim 14.6$ (8.3 kpc). The choice of 0.6 mag as the bin size is derived from the average errors in DM. These errors mainly originate in the uncertainties of spectral type and luminosity class determinations combined with the uncertainties in the corresponding absolute magnitude calibrations. Those two apparent concentrations in the distribution of DM seem to be coincident with those found by O95, namely Ru 55 A at 4.2 kpc and Ru 55 B at 7.5 kpc, but the stars belonging to each group are not exactly the same. Our observed sample has 18 stars in common with O95 showing $DM > 12.8$. Among these, both O95 and this study agree on four stars from Ru 55 A and seven stars
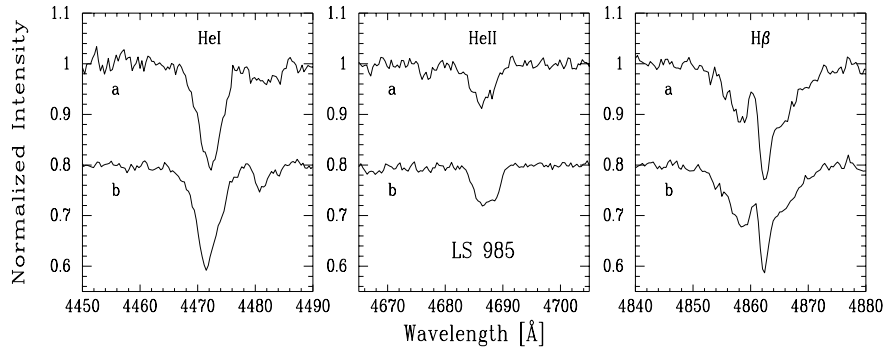
Figure 3. He I 4471 Å, He II 4686 Å and Hβ in the spectrum of the double-lined O-type binary LS 985 at two different observing dates: (a) JD 244 9369.698, and (b) JD 244 9382.601.
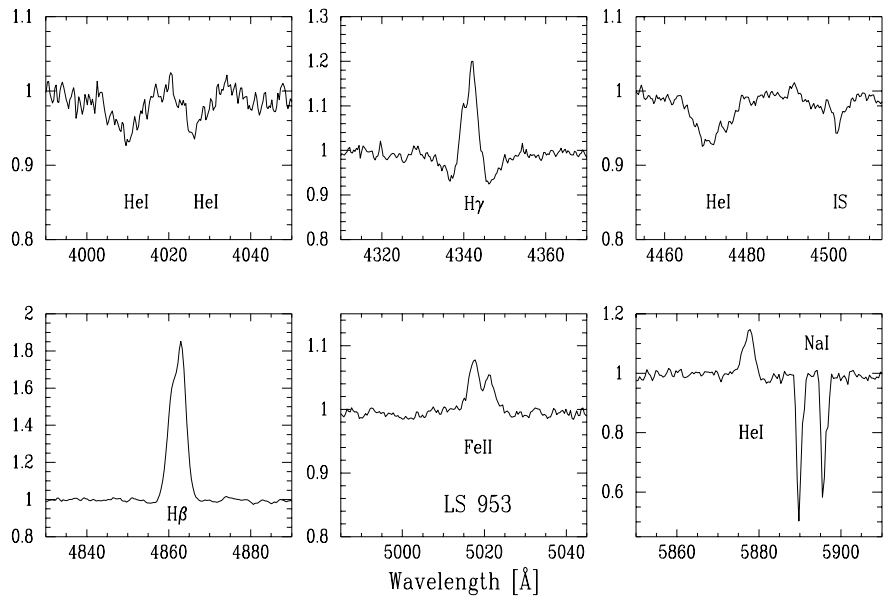
Figure 4. Selected absorption and emission lines in the spectrum of the peculiar Be star LS 953.

from Ru 55 B. The other seven would be assigned in this study to a different group than O95. Taking into account the errors involved in the DM derived from spectroscopy ($\sigma \sim 0.6$ mag) and that the two apparent concentrations are only 1.2 mag apart in DM, the physical reality of each grouping is not well established. Besides,
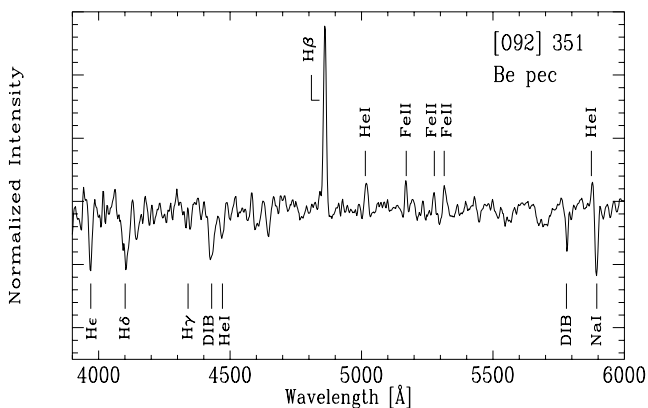
Figure 5. Low-resolution spectrum of the peculiar Be star [O92] 351.
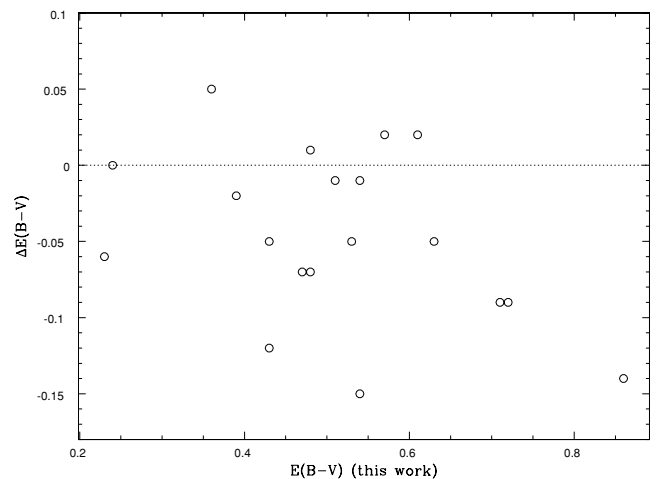
Figure 6. Comparison between *B–V* colour excesses: differences are calculated as those determined from spectroscopic intrinsic colours minus those from photometric data alone. The majority of points showing negative values suggest a slight overestimation of the colour excess by the photometric method.
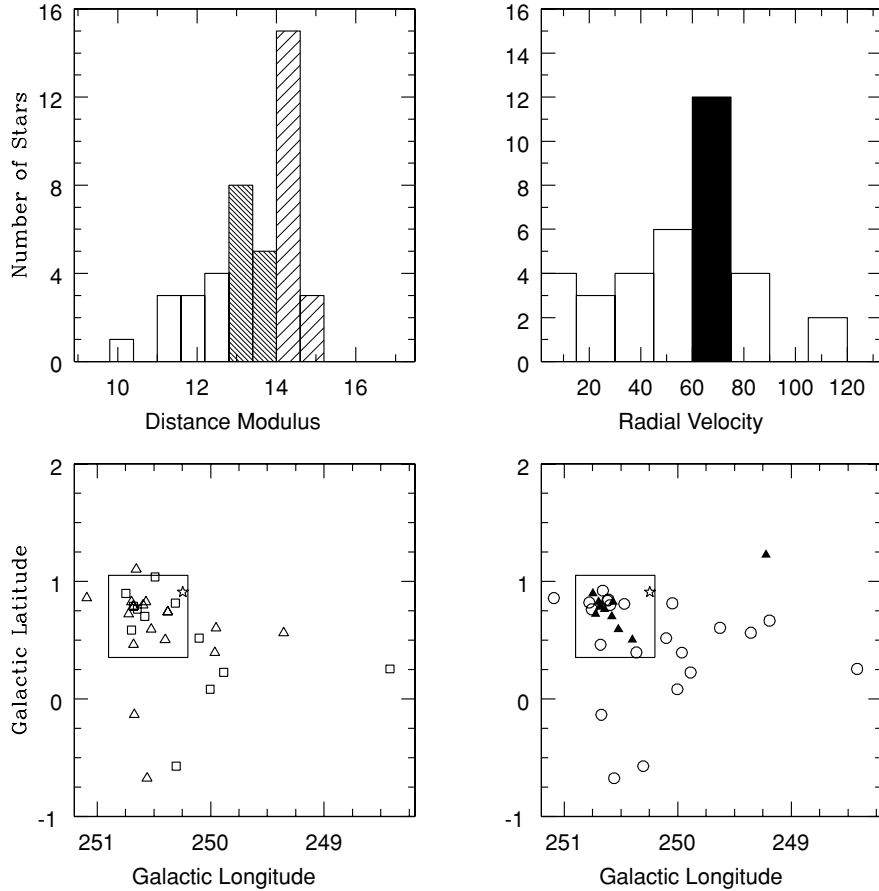
Figure 7. In the upper left-hand panel we show the distribution of the DM of the OB stars in the observed sample. The tightly stripped bins are those stars with $12.8 < DM < 14.0$, and loosely stripped bins are those stars $14.0 < DM < 15.2$, labelled with squares and triangles in the lower left-hand panel, respectively. In the upper right-hand panel we show the LSR radial velocity distribution of the OB stars in the same observed sample. The notorious peak (in dark colour) at about 70 km s^{-1} suggests a stellar group sharing common kinematics. The lower right-hand panel plots again the spatial distribution, where black triangles indicate stars in the 70 km s^{-1} bin, and open circles the rest of the sample. A small box in this panel highlights the concentration of the kinematical sample. The O-type binary LS 985 is marked with a star.

both groupings are undistinguishable from the point of view of the radial velocity, colour excess, or spatial distribution. The latter can be seen in the lower left-hand panel of Fig. 7, where squares identify stars with $12.8 < DM < 14.0$ and triangles those with $14.0 < DM < 15.2$. O95 pointed out that stars belonging to Ru 55 A and Ru 55 B have similar colour excess, a fact that she attributed to most of the absorbing material being located in front of the nearest group (Ru 55 A).

The large uncertainties present in the individual stellar distances and the small number of objects make the identification of a stellar cluster towards this region extremely difficult using stellar DM as the only tool. In what follows we include kinematical information from the stars and the interstellar gas, to better constrain the existence of a cluster – or association – of stars.

4.2 Stellar kinematics

Fig. 7 (upper right-hand panel) shows the distributions of estimated radial velocities for *all* of the observed stars in a histogram. The choice of 15 km s^{-1} wide bins is a compromise value between resolution and keeping a representative number of elements per bin. The concentration of stars at the bin ranging from 60 to 75 km s^{-1} is in accordance with the result just described in the previous section.

These stars are plotted in dark colour in the DM distribution (upper left-hand panel).

The lower right-hand panel of Fig. 7 shows the spatial distribution of the observed stars with measured radial velocity. Triangles represent the stars lying in the 60–75 km s^{-1} bin. This figure suggests a concentration of early-type stars sharing similar radial velocity at the same distance modulus and spatially grouped, as marked by the small box within the surveyed area. In Section 5 we will further discuss the importance of such a concentration when combined with the H I distribution.

4.3 H I distribution

In order to investigate the distribution of the interstellar gas in the vicinity of the cluster, we analysed a series of H I emission images at positive velocities.

The neutral gas images show a H I cavity centred at $(l, b, v) \simeq$ (249°9, +1°7, +65 km s^{-1}) of about 1°0 in radius. Fig. 8 displays the mean brightness temperature T_b within the velocity interval 61.5 to 68.3 km s^{-1}, where the H I structure is more clearly defined. Ru 55, which is indicated by a triangle, appears projected close to the border of the cavity. The minimum is encircled by a thick shell open opposite the galactic plane. The H I cavity and envelope are also
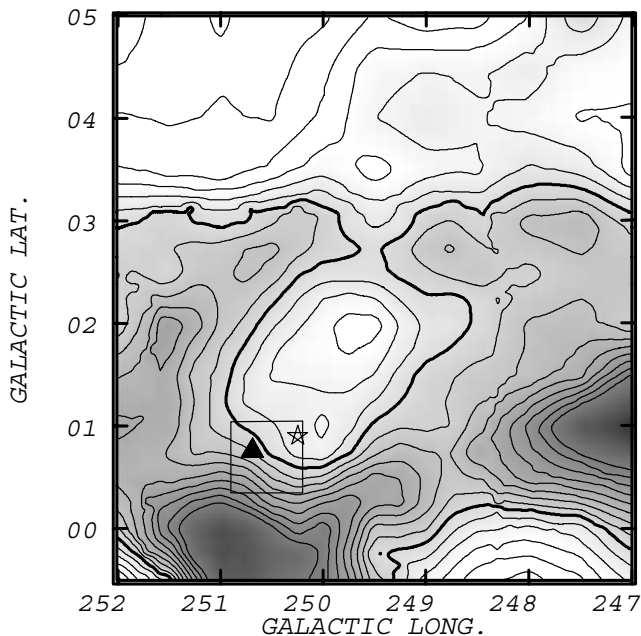
Figure 8. Mean brightness temperature within the velocity interval 61.5–68.3 km s^{-1} showing the H I cavity probably associated with Ru 55. The grey-scale corresponds to 12–55 K. Contour levels are drawn from 6 to 44 K in steps of 2 K. The highest-T_b (18 K) contour, plotted with a thicker line, marks the outer border of the H I minimum. The triangle marks the position of the nucleus of the stellar group, and the star indicates the position of LS 985.

visible in the map at $l = 250°$ on the Green Bank H I survey (Burton 1985). This last map illustrates that the void does not represent an H I minimum in the Local (0) and Perseus (+I) interarm region.

Analytical fitting to the circular Galactic rotation model by Brand & Blitz (1993) predicts that material moving at ∼65 km s^{-1} should be located at a kinematical distance of 7.0 kpc. A similar result (7.5 kpc) can be derived from the expressions by Clemens (1985), which are based on CO observations. On the other hand, based on the *observed* velocity field of the Galaxy derived by Brand & Blitz (1993), which takes into account the presence of non-circular motions, we estimate that gas at this velocity should be placed at a kinematical distance of 6 kpc. We adopt a mean kinematical distance of 6.8 ± 1.5 kpc.

The distance uncertainty, likely to be a lower limit, stems from the uncertainty in the distances of the H II regions, typically larger than 25 per cent, used by Brand & Blitz to derive the observed galactic velocity field. The adopted kinematical distance is in agreement, within the errors, with the distance derived for the cluster using spectroscopic parallaxes (see Section 5).

4.3.1 Parameters of the main minimum

To derive a few parameters that may help us to quantitatively define the H I minimum, we have followed the procedure outlined by Arnal & Roger (1997). Bearing in mind the definitions made in that paper, we have adopted as the outer border of the H I minimum the highest-T_b close contour line (18 K). Likewise, the major and minor axes of the H I cavity are given by d_M and d_m, respectively. Due to projection effects, both axes are likely to be lower limits. By placing the minor axis halfway along the major axis and perpendicular to it, the symmetry centre of the minimum is defined as the crossing

Table 2. Parameters of the H I feature.

Symmetry centre *(l, b)*	249°9, +1°7
Velocity range v_1, v_2 (km s^{-1})	+62, +72
V_{sys} (km s^{-1})	+65
Kinematical distance (kpc)	6.8±1.5
d_M (pc)	250±40
d_m (pc)	170±28
Total atomic missing mass (10^3 M$_\odot$)	11–36
Volume density n_0 (cm^{-3})	0.1–0.4
Velocity extent $\triangle V$ (km s^{-1})	10

point of the axes. The properties of the cavity are given in Table 2. Linear dimensions, mass and volume density are derived assuming a distance of 6.8 kpc.

We would like to stress that the velocity extent quoted in Table 2 corresponds to the velocity range where the H I depression remains detectable from an observational point of view. Very likely, it represents a lower limit to the real velocity extent of the H I void, because 'extreme'-velocity gas associated with the cavity could be missed, owing to confusion effects. The systemic radial velocity, V_{sys}, represents the velocity at which the H I deficiency achieves its maximum angular extent.

For the sake of completeness, we would like to remind the reader that the lower limit for the total atomic mass quoted in Table 2 represents the *minimum amount* of atomic mass needed to 'fill in' the observed H I minimum up to the 18-K contour. In going from neutral hydrogen mass to total atomic mass, we have assumed solar abundances by multiplying the H I mass by 1.36. This mass limit is equivalent to the definition of M_{HI}^{miss} in Arnal & Roger (1997). On the other hand, since the H I minimum is detected *by contrast* with the surrounding H I emission, an alternative estimate of the missing mass could be derived from a calculation of the H I mass needed to make the H I minimum *undetectable with respect to its average surrounding* atomic hydrogen emission. This last estimate is very likely an upper limit and corresponds to the definition of M_{HI}^{un} in Arnal & Roger (1997). These mass extremes are those given in Table 2 as lower and upper limits for the *total* atomic missing mass. The neutral hydrogen emission was assumed to be optically thin. A lower (higher) limit for the density prevailing in the atomic gas before the H I minimum was created is obtained as the lower (upper) limit of total atomic missing mass divided by the volume of the H I minimum, assumed to be an ellipsoid with major axis d_M and the other axes equal to d_m.

Finally, a rough estimate of the kinetic energy of the H I feature can be obtained as $E_k = M V_{exp}^2 / 2$, where M equals the total atomic missing mass. A lower limit to the expansion velocity of 5 km s^{-1} can be inferred from the velocity extent of the H I cavity (Table 2). As this value is a lower limit to the true expansion velocity, we adopted the velocity corresponding to the turbulence motions in the interstellar medium (ISM; i.e. ≈8 km s^{-1}) as the expansion velocity of the structure. Taking into account these values, the kinetic energy turns out to be $E_k = (0.7–2.3) \times 10^{49}$ erg.

5 DISCUSSION

5.1 Distance to the cluster

The knowledge of spectral types allows a better characterization of the stellar population, mostly regarding its evolutionary stage. The presence of an O9 V + O9.5 III star suggests an age of 5×10^6 yr

(Massey 1998), considering for the binary pair an evolutionary path not very different from that of a single O9 V star. Early B supergiants might have evolved from late O-type stars in similar time-scales.

In order to identify the existence of a cluster (or association) in the direction of Ru 55, we must analyse the data presented above and seek evidence that locates stars in a particular place in our Galaxy. The improved spectral classification presented here allows us to identify a considerable number of early type stars in the region. However, this information only describes a projected view. We can attempt to disentangle it using the LSR radial velocity as a distance indicator, as there is no ambiguity (although rather large errors) when determining distances from the rotation curve in the third quadrant. The colour excess observed for each star can also be used to estimate relative distances (from the observer) for stars in the sample. This relies on the assumption that the interstellar material responsible for reddening piles up smoothly as distance increases, as there are no notorious clouds or strong filaments towards the observed direction. We have also derived individual DM to each star by estimating their absolute magnitude from its spectral type (spectroscopic parallax). This method, although straightforward, is very sensitive to uncertainties in the classification process.

We have checked for correlations between these three independent distance indicators. Fig. 9 shows the relation between LSR radial velocity and colour excess. The plot shows that points do not fill the plane uniformly, as relatively lower radial velocities correspond to smaller colour excesses (and the same holds for larger values of V_r and $E(B-V)$). The somewhat large scatter of the whole sample is reduced if we only consider stars that do not show evidence of radial velocity variations (filled circles). A similar trend is also seen in Fig. 10 where we have plotted the same radial velocities now against the spectroscopic DM. However, the error bars along the x-axis are much wider, as small uncertainties in the spectral classification lead to large errors in the absolute magnitudes for early-type stars.

Notwithstanding the uncertainties described we can attempt to measure the distance to stars that show similar radial velocities (i.e.
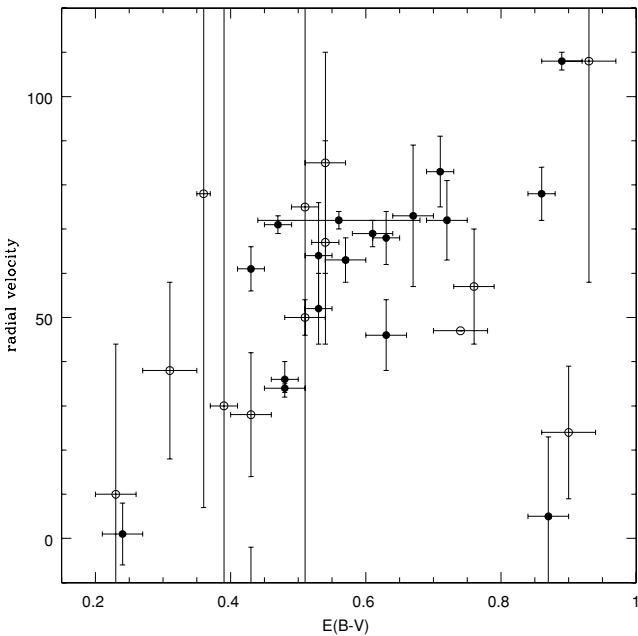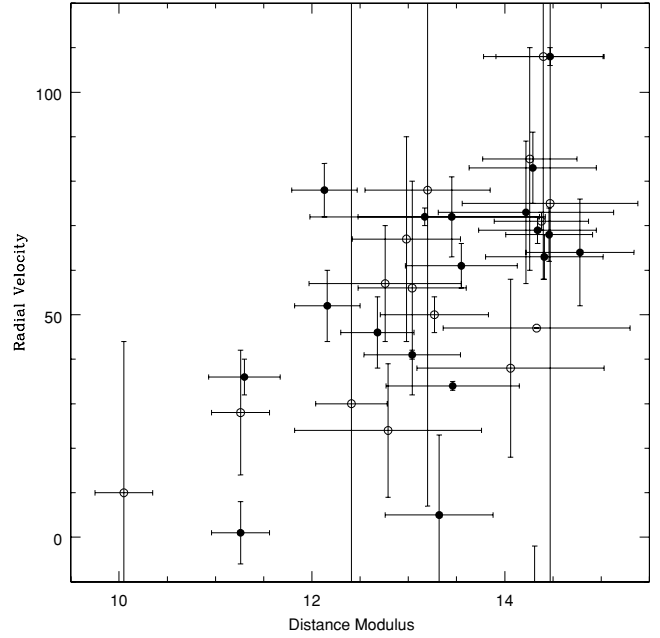

Figure 10. Plot of the LSR radial velocity measured for stars in Ru 55 and their DM determined from spectroscopic absolute magnitudes. Symbols are identical to those in Fig. 9.

stars included in the $\sim$70 km s^{-1} bin in Fig. 7). In order to work with the most reliable subset we only included in our calculation those stars that showed no variations in their radial velocity determined with high-resolution spectroscopy (nine stars). The average distance modulus derived for these stars is 13.95 ± 0.50, resulting in a distance of 6.2 ± 1.4 kpc which is consistent with the distance derived from H I kinematics. Thus, within observational errors, the agreement both in distance and position between the H I structure and the most reliable open cluster members enables us to propose that it is very likely that both objects are physically related.

5.2 Origin of the cavity

It is worth investigating if the cavity could have originated in the action of the stellar winds of massive stars belonging to Ru 55. The mechanical energy necessary to blow the observed H I cavity can be estimated from the energy conserving bubble model (Weaver et al. 1977) as $E_w^{\mathrm{min}} = 5E_k = (0.4-1.2) \times 10^{50}$ erg. This value can be considered as a lower limit as the observed ratio between the mechanical energy supplied by the stellar wind E_w and the kinetic energy E_k of the shell is generally larger than 10 (Cappa & Herbstmeier 2000).

The mechanical energy E_w supplied by the massive stars of Ru 55 can be estimated as $E_w = t_d L_w$, where $L_w = \frac{1}{2} \sum_i \dot{M}_i V_{w,i}^2$, with $\dot{M}_i$ and $V_{w,i}$ being the mass-loss rates and terminal velocities of the stars and t_d the dynamical age of the interstellar bubble.

The last parameter is defined as $t_d = 0.55\, R/V_{\mathrm{exp}}$, where the constant represents a mean value between the energy and momentum conserving cases (Koo & McKee 1992) and R is the radius of the bubble. Adopting $R(=\sqrt{d_M d_m}/2) = 100 \pm 15$ pc and $V_{\mathrm{exp}} = 8$ km s^{-1}, we find $t_d \simeq (7 \pm 1) \times 10^6$ yr, in good agreement with the age estimate derived for the earliest star in the cluster.

An estimate of the mechanical luminosity L_w was derived by taking into account the contribution from stars having spectral types earlier than B3 and radial velocities compatible with that of the

Figure 9. Plot of the LSR radial velocity measured for stars in Ru 55 and their $B-V$ colour excesses determined from spectroscopic intrinsic colours. Symbols identify stars which show radial velocity variations (open circles) and those which do not (filled circles).

cavity (see Table 1). Their mass-loss rates were estimated from the expression by Lamers & Leitherer (1993), while their terminal velocities were adopted from Prinja, Barlow & Howarth (1990). In the binary system LS 985 [$(l, b) = (250°.25, +0°.91)$], which is 68 pc away from the nucleus of Ru 55, reside the O-type stars in the stellar group. The position is indicated in Fig. 8 as an asterisk. According to evolutionary tracks, the current O9.5 III star may have spent $\sim 5 \times 10^6$ yr in the main sequence as an O8 V star (Massey 1998). We adopted typical stellar wind parameters for O8 V and O9 V stars. The mechanical luminosity derived for the binary system is 2.5×10^{35} erg s^{-1}, similar to the mechanical luminosity (2.1×10^{35} erg s^{-1}) estimate corresponding to the B-type stars in the stellar grouping. Assuming that LS 985 spent 5×10^6 yr in the main sequence, the total mechanical energy supplied by the stellar group to the ISM amounts to 0.7×10^{50} erg. Thus, the energy supplied by Ru 55 is barely enough to blow the observed cavity.

There are other early-type candidate stars projected on to the minimum at a distance compatible with that of Ru 55 and the H I cavity, namely LS 976 [$(l, b) = (250°.10, 0°.52)$], 977($249°.80$, $0°.82$), 992($249°.57$, $1°.55$), 1004($249°.67$, $1°.75$), 1008 ($250°.27$, $1°.41$), 1009($251°.09$, $0°.86$) and 1015($250°.89$, $1°.28$). Distances to these stars were obtained from the calibration in absolute magnitudes by Reed & Nyman (1996) and visual absorptions in the range $A_v = 1.5$–2.5 mag. Although luminosities derived using this calibration suggest that altogether they might contribute up to 10 per cent of the total energy budget, our spectral data reveal that several of them actually have significantly lower luminosities.

Two other cluster candidates, namely Ru 54 and Ru 58, were noted by Alter et al. (1970) in the direction of the H I cavity. However, they have less chance of being able to blow such a cavity as they seem to lack OB stars. None the less, we have obtained a few spectra for the brightest stars in the Ru 58 field, but found later-type stars which have LSR radial velocity close to zero, suggesting they are foreground stars.

5.3 LS 985 circumstellar activity

Some shells of H I surrounding interstellar bubbles possess counterparts at radio continuum and infrared wavelengths (van der Werf & Higgs 1990; Cappa & Herbstmeier 2000) displaying a similar morphology to that observed in the H I line. An inspection of the total power 'large-scale' component image of the 2.47-GHz continuum survey (Duncan et al. 1995) shows the presence of a $5°.9$ long and $2°.3$ wide emission feature partially projected on to the H I cavity. A closer look at the correspondence (on the plane of the sky) between the H I structure displayed in Fig. 8 and the continuum distribution does not show the sort of spatial correlation that we would expect if they were physically related. Hence, we conclude that no extended radio continuum feature is related to the cavity. With regard to the large-scale IR emission, a similar conclusion can be drawn after analysing the 60- and 100-µm *IRAS* images.

Because massive stars have a large output of photons shortward of the Lyman continuum limit ($\lambda \leqslant 912$ Å) they are likely to be surrounded by regions of ionized gas. Following Schaerer & de Koter (1997) the total number of ionizing photons, N_{Lyc} emitted by LS 985 is $N_{\mathrm{Lyc}} \sim (9.2^{+8.7}_{-5.3}) \times 10^{48}$ s^{-1}. The quoted uncertainties are derived under the assumption that the spectral types are accurate to within one spectral class. A look at the total power 'small-scale' images of the 2.47-GHz survey shows, besides scatter emission all over the area, a region of weak and patchy emission that is mostly confined within a circle of $\sim 0°.9$ in radius centred on LS 985 (Fig. 11). The measured flux density is 6.3 ± 1.4 Jy and, following Chaisson
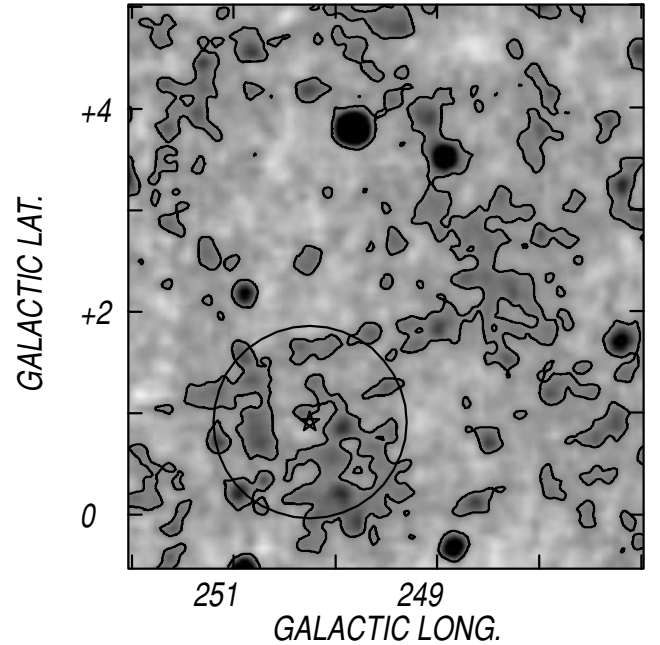

Figure 11. Total power 'small-scale' structure image at 2.47 GHz. The grey-scale goes from -50 (light grey) to 300 (dark grey) mJy beam^{-1}. The contour level is 85 mJy beam^{-1}. The star marks the position of LS 985 and the circle delineates an area of $0°.9$ in radius.

(1976), the number of ionizing photons needed to keep ionized an optically thin H II region located 6.8 kpc away is $N_{\mathrm{Lyc}} \sim (2.4 \pm 1.4) \times 10^{49}$ s^{-1}. This figure agrees, within errors, with the number of ionizing photons emitted by LS 985. Owing to this, the low-level continuum emission observed around LS 985 may represent an H II region powered by this binary system. As LS 985 itself may be located within the low-density cavity shown in Section 4.3.1, the observed H II region may result from the impact of the high-energy ionizing photons on to the H I shell engulfing the interstellar bubble, providing thus further evidence in favour of a physical association between the H I cavity and LS 985. The reality of the low-level emission around LS 985 can also be judged from Fig. 12 which shows the results of a ring integration carried out on the 'small-scale' images of the 2.47-GHz continuum survey, on 5-arcmin wide annuli centred on LS 985. The abscissae represent angular distance from
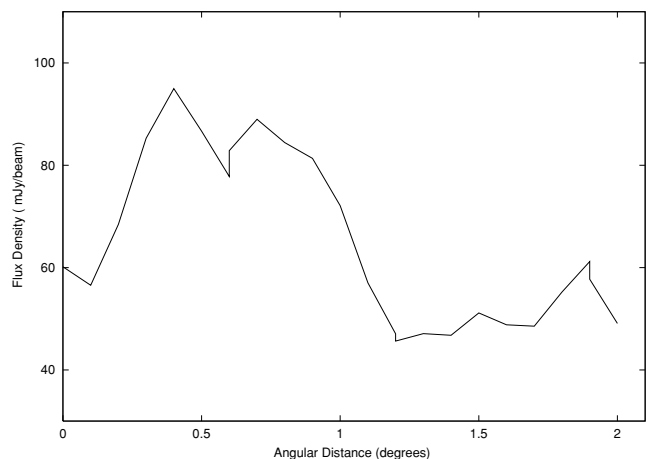

Figure 12. Ring integrations carried out on the image displayed in Fig. 11.

LS 985 expressed in units of degree, while the ordinates are the mean continuum flux density within a given annulus. Clearly, the continuum emission level within a circle of radius $0.°9$, $S = 79 \pm 11$ mJy beam^{-1}, is well above the mean emission of the surrounding region, namely $S = 51 \pm 5$ mJy beam^{-1}.

6 CONCLUSIONS

Combining new photometric and spectroscopic information in the optical range, together with radio wavelength data, we have searched for the presence of a stellar cluster (or association) through the Puppis window.

From the radial velocity data – backed by a strong correlation with colour excesses – we have identified a stellar association which shares a common LSR radial velocity ($\sim$67 km s^{-1}) with a H I depletion. Star LS 985, found to be an early-type spectroscopic binary, should have had enough energy to be the major star responsible for blowing the cavity. Furthermore, from the expected evolutionary stages of the earliest-type stars, we estimate an age of the cluster of $\sim$5 $\times$ 10^6 yr. This is in good agreement with the cavity evolution time-scales and LS 985 seems to be triggering the formation of an H II region within the depletion.

The errors involved in individual DM determinations do not allow a clear differentiation between both groups identified by O95. Moreover, we were not able to identify any star grouping that could be linked to their Ru 55 A cluster.

Unfortunately, Ru 55 lies too far to make use of Tycho-2 (Høg et al. 2000) proper motions to determine spatial velocities. Typical errors for stars in this region are 2.5 mas yr^{-1}, which correspond to more than 70 km s^{-1} at the OB association distance. We expect that future missions, such as GAIA, will provide useful proper motion information.

We can therefore suggest the use of Ru 55 as a spiral structure tracer. At a distance of about 6 kpc – independently estimated from spectroscopic parallaxes and gas kinematics – in the [$(l, b) = (250°, -1°)$] direction we place it as an extension of the Perseus arm.

REFERENCES

Alter J., Ruprecht J., Vanysek V., Balazs B. A., 1970, in Alter G., Balazs B., Ruprecht J., eds, Catalogue of Stars Clusters and Associations, 2nd edn. Akademiai Kiado, Budapest
Arnal E. M., Roger R. S., 1997, MNRAS, 285, 253
Brand J., Blitz L., 1993, A&A, 275, 67
Burton W. B., 1985, A&AS, 62, 365
Cappa C. E., Herbstmeier U., 2000, AJ, 120, 1963
Chaisson E. J., 1976, in Avrett E. H., ed., Frontiers of Astrophysics. Cambridge, Harvard Univ. Press, p. 259
Clemens D. P., 1985, ApJ, 295, 422
Cutri R. M. et al., 2000, Explanatory Supplement to the 2MASS Second Incremental Data Release. Caltech, Pasadena
de Zeeuw P. T., Hoogerwerf R., de Bruijne J. H. J., Brown A. G. A., Blaauw A., 1999, AJ, 117, 354
Dodd R. J., Ellery L. A., 1980, MNRAS, 193, 895 (DE80)
Dommanget J., Nys O., 2002, Observations et Travaux, Societe Astronomique de France. ftp://cdsarc.u-strasbg.fr/cats/I/269
Duncan A. R., Stewart R. T., Haynes R. F., Jones K. L., 1995, MNRAS, 277, 36
Garrison R. F., Hiltner W. A., Schild R. E., 1977, ApJS, 35, 111
Høg E. et al., 2000, A&A, 355, L27
Houk N., 1982, Michigan Spectral Survey. Univ. Michigan, p. 3
Johnson H. L., 1966, ARA&A, 4, 193
Koo B. C., McKee C. F., 1992, ApJ, 388, 93
Lamers H. J. G. L. M., Leitherer C., 1993, ApJ, 412, 771
Landolt A. U., 1992, AJ, 104, 340
Massey P., 1998, in Aparicio A., Herrero A., Sanchez F., eds, VIII Canary Islands Winter School of Astrophys., Stellar Astrophysics for the Local Group. Cambridge Univ. Press, Cambridge, p. 95
Orsatti A. M., 1992, AJ, 104, 590 (O92)
Orsatti A. M., 1995, AJ, 110, 1728 (O95)
Prinja R. K., Barlow M. J., Howarth I. D., 1990, ApJ, 361, 607
Reed B. C., Nyman M. A., 1996, PASP, 108, 395
Schaerer D., de Koter A., 1997, A&A, 322, 598
Schmidt-Kaler Th., 1982, in Shaifers K., Voigt H. H., eds, Landolt-Börnstein, New Series, Group VI, Vol. 2/b. Springer-Verlag, Berlin
Stephenson C. B., Sanduleak N., 1971, Pub. Warner & Swasey Obs., 1, 1
Stetson P. B., 1987, PASP, 99, 191
Stetson P. B., Fitzgerald M. P., 1985, AJ, 90, 1060
van der Werf P. P., Higgs L. A., 1990, A&A, 235, 407
Walborn N. R., Fitzpatrick E. L., 1990, PASP, 102, 379
Weaver R., McCray R., Castor J., Shapiro P., Moore R., 1977, ApJ, 218, 377
Williams D. R. W., 1973, A&AS, 8, 505

This paper has been typeset from a TEX/LATEX file prepared by the author.